Identifying the sources of CO_2 in carbonic springs in the Albuquerque-Belen Basin

Valerie Blomgren, Amy Williams, Laura Crossey, Karl Karlstrom, and Fraser Goff

2016, pp. 419-427. https://doi.org/10.56577/FFC-67.419

in:

Guidebook 67 - Geology of the Belen Area, Frey, Bonnie A.; Karlstrom, Karl E. ; Lucas, Spencer G.; Williams, Shannon; Zeigler, Kate; McLemore, Virginia; Ulmer-Scholle, Dana S., New Mexico Geological Society 67th Annual Fall Field Conference Guidebook, 512 p. https://doi.org/10.56577/FFC-67

This page is intentionally left blank to maintain order of facing pages.

New Mexico Geological Society Guidebook, 67th Field Conference, Geology of the Belen Area, 2016, p. 419-427.

IDENTIFYING THE SOURCES OF CO_2 IN CARBONIC SPRINGS IN THE ALBUQUERQUE-BELEN BASIN

Valerie Blomgren[1], Amy Williams[2], Laura Crossey[1], Karl Karlstrom[1], and Fraser Goff[1]

[1] University of New Mexico Department of Earth and Planetary Sciences, Albuquerque, NM 87131
[2] Towson University, Department of Physics, Astronomy, and Geoscience, 8000 York Road, Towson, MD 21252

Abstract—Understanding groundwater resources in the Albuquerque basin region requires an understanding of the geochemistry of carbonic springs and potential mixing among different water sources. Carbonic springs are defined as high P_{CO2} springs (P_{CO2} >10-1.8). This paper evaluates the sources of the high dissolved CO_2 in these springs by summarizing the geochemistry of carbonic springs found along faults of the Rio Grande rift. Major ion chemistry helps define chemical characteristics of endogenic (deeply sourced) fluids entering the groundwater system and their variable mixing with epigenic waters (meteoric recharge). We also use major ion water chemistry analyses to estimate the percentage of CO_2 derived from dissolution of carbonates (both rock and minerals) (C_{carb}) in groundwater. We then use carbon isotopes to estimate the percentage of the remaining external CO_2 (C_{ext}) that was derived from organic material such as soil gas (C_{org}) plus endogenic CO_2 that is from deeply derived sources (C_{endo}). The results show a high percentage of endogenic components in the west flank of the Rio Grande rift spring waters with a range of 17.5 - 74.8% C_{endo} (mean value of 55.3%±19.8%). We analyzed dissolved gases to illustrate a spectrum of mixing between air and air-saturated groundwater with helium-rich deeply sourced fluids. The high endogenic CO_2 in springs and travertines that occur within the Rio Grande rift at San Acacia and along much of the western rift faults from Socorro to I-40 is interpreted to reflect degassing of magmatic volatiles from the Socorro magma body. The wide distribution of springs suggests that similar waters may be cryptically entering Santa Fe Group aquifers from below and affecting water quality by adding salinity and trace metals as well as deeply sourced volatiles. These endogenic inputs are tepid (up to 26°C) and have geochemical similarities to geothermal waters. The variation in hydrochemistry of the Albuquerque basin can be attributed in part to mixing of endogenic fluids with other groundwater and has implications for future management of groundwater resources.

INTRODUCTION

Carbonic springs are defined as high P_{CO2} springs, with the lower limit of P_{CO2} in this study of $10^{-1.8}$ which is nearly 2 orders of magnitude higher in CO_2 than waters equilibrated with air which have $P_{CO2} = 10^{-3.5}$. Distinctive carbonic springs discharge in the Albuquerque basin along fault and fault zones of the Rio Grande rift (Fig. 1). These springs often produce large volume travertine (Priewisch et al., 2014). A major question involves the source of the CO_2. This is important because the high total CO_2 (HCO_3 and CO_2 gas) is also associated with high salinity, high metal content, and the presence of mantle–derived helium (Crossey et al., 2011) as part of deeply sourced (endogenic) fluid end members that mix within the aquifer system. Williams et al. (2013) presented a hypothesis that diverse water quality and hydrofacies of springs in the Sevilleta Game Refuge and Albuquerque basin can be explained by mixing of meteoric recharge (epigenic) waters with deeply sourced (endogenic) waters. This hypothesis is summarized and further tested in this paper.

Several recent papers have highlighted the importance of understanding mixing of different fluids within the aquifer as an explanation for variable groundwater composition across the Colorado Plateau region (Newell et al., 2005; Crossey et al., 2006, 2009, 2011; Williams et al., 2013). Similarly, groundwater inputs are noted to have an important influence on surface water quality. For example, endogenic inputs can explain the abrupt increase in salinity of the Rio Grande when it passes San Acacia (Mills, 2003; Hogan et al., 2007; Williams et al., 2013). However, the sources of the salts and the CO_2 remain poorly understood and there may be more than one type of endogenic fluid. For example, Cl/Br ratios suggest that abrupt increase in salinity of the Rio Grande at San Acacia and San Marcial cannot be explained by agricultural inputs, but could reflect upwelling of basin brines (Mills, 2003; Hogan et al., 2007), inputs from the mantle (Newell et al., 2005; Williams et al., 2013), and/or mixing of geothermal fluids during ascent from depth.

The goal of this paper is to explore the sources of CO_2 in the carbonic springs of the Albuquerque basin. We analyze multiple geochemical tracers in groundwater to help recognize and unravel the components from meteoric recharge, water-rock interaction along flow paths, and variable mixing of different groundwater sources such as geothermal fluids. This paper presents major ion chemistry, stable isotope data, and dissolved gas tracers. We also explore the possibility that the chemical characteristics of endogenic fluids (elevated salinity, CO_2 gas, and mantle-derived helium) can be explained by input of magmatic volatiles from the Socorro magma body. If so, this would suggest tectonic interconnections between deep fluids, travertines, fault conduits, and magmatic volatiles in the Albuquerque basin of the Rio Grande rift (Fig. 2).

We also integrate our data with a previous study of springs of the Lucero Uplift (Goff et al., 1983) that was designed to test the geothermal potential of springs along the west margin of the Rio Grande rift and adjacent Lucero Uplift. These workers noted that this region had an unusual set of mesothermal springs (12 to 26°C) that were associated with a region of Quaternary faulting, volcanism, regional high heat flow, and the potential for geothermal reservoirs (Callendar and Zillinski, 1976; Train-

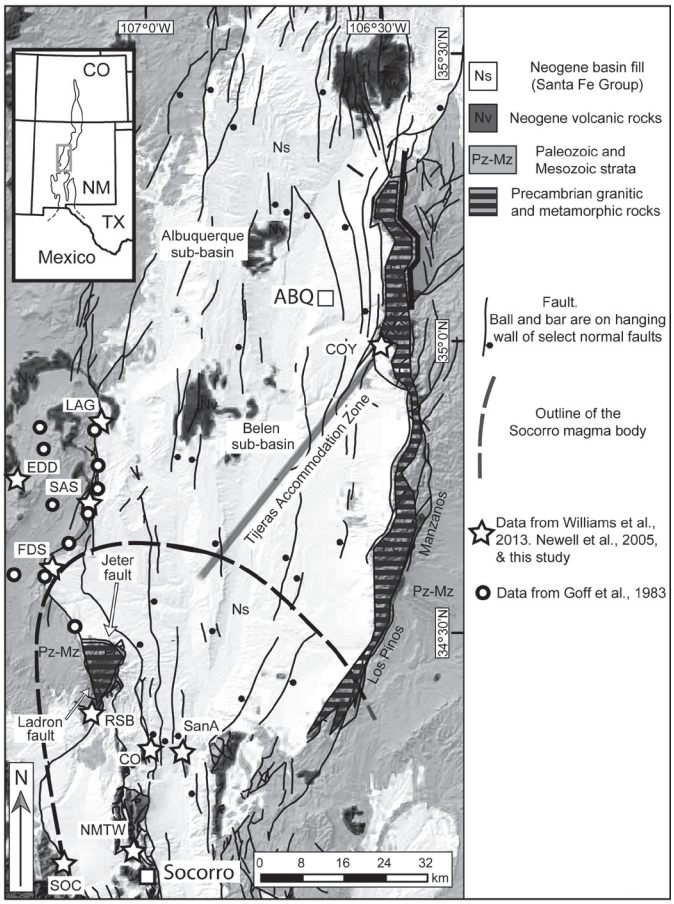

FIGURE 1. Digital elevation model of the Rio Grande rift showing rift-bounding faults. The Socorro magma body underlies the area outlined by the dashed line at ~19-km depth. Fault-related carbonic springs analyzed are Coyote (COY), Laguna Pueblo (LAG), Eddleman (EDD), Salado Arroyo (SAS), Four Daughters (FDS), Rio Salado Box (RSB), Canyon del Ojito (CO), San Acacia (SanA). The Socorro spring (SOC) and New Mexico Tech Well (NMTW) are located on the southern end of the study site. Spring samples from Goff et al. (1983) are shown in hollow circles on the western side of the rift.

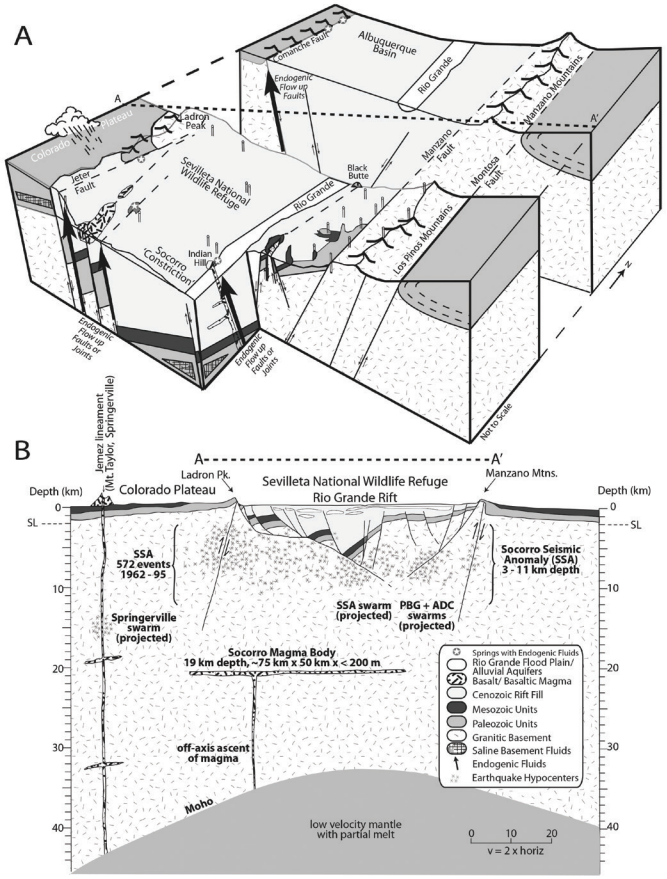

FIGURE 2. Block diagram (from Williams et al., 2013) of the Rio Grande rift illustrating endogenic fluids flowing upwards along rift-related normal faults (large black arrows). Rift flank meteoric recharge flows from both sides of the rift into the valley and then southward (small black arrows). The Colorado Plateau is located to the west of the study area and influences the meteoric recharge into the basin.

er and Lyford, 1979). One study had reported calculated subsurface reservoir temperatures of >100°C using Na-K-Ca chemical geothermometers (Fournier and Truesdell 1973).

GEOLOGIC BACKGROUND

The Albuquerque basin is within the central portion of the Rio Grande rift that has been undergoing extension in the last 25-30 Ma (Chapin and Cather, 1994; Russell and Snelson, 1994; Keller and Baldridge, 1999) and is still active (Ricketts et al., 2014). The basin is composed of half grabens bound by normal faults; the west-dipping Sandia-Manzano range-bounding faults on the east side of the northern part of the Albuquerque basin and the east-dipping Jeter and Santa Fe fault systems on the west side of the southern part of the basin. The change in half graben asymmetry on the opposite sides of the Albuquerque basin requires an accommodation zone in the central part of the basin (Fig. 1) that Grauch et al. (2013) and Ricketts et al. (2014) considered to be a distributed zone of *en echelon* anticlines rather than a single fault zone (c.f. Lewis and Baldridge, 1994).

Springs described in this paper are listed in Tables 1-4 and shown in Figure 1. One set occurs along the western rift-bounding faults. From north to south, these are: Laguna Pueblo (LAG), Salado Arroyo Spring (SAS), Four Daughters Spring (FDS), Rio Salado Box springs (RSB), Canyon del Ojito spring (CO), New Mexico Tech Well (NMTW) and Socorro spring (SOC). Eddleman Spring (EDD) is on the Colorado Plateau just west of the rift boundary. San Acacia spring (SanA) is along the Cliff fault in the center of the rift. Coyote springs (COY) are along the eastern rift boundary at the intersection of the rift bounding Sandia fault zone and Tijeras fault zone. Water and gas analyses of most of the above springs were compiled from Williams et al. (2013) and Newell et al. (2005). These authors also reported helium isotope data (R_C/R_A) for these springs ranging from 0.256 to 1.907 R_A indicating that 3-15% of the helium in these springs was derived from the mantle. New water chemistry data is presented for Laguna Pueblo spring and new gas data for Four Daughters, New Mexico Tech Well and Socorro spring.

Because springs are located along rift bounding faults, all of the springs have the potential to derive meteoric recharge from adjacent uplifted rift flanks, from the shallow Santa Fe

TABLE 1. Spring parameters.

ABQ Basin Group	Spring	Sample Date	Lat	Long	Temp°C	pH	Conductivity (µS)	Source
Canyon del Ojito Spring	Canyon del Ojito Spring	08.07.08	34.260700	-106.975260	22.5	9.12	1640	Williams et al., 2013
Canyon del Ojito Spring	Canyon del Ojito Spring	06.23.09	34.260700	-106.975260	22.4	8.8	1535	Williams et al., 2013
East springs	Canyon Well	05.29.09	34.314720	-106.715550	19.7	7.39	902	Williams et al., 2013
East springs	Cibola Spring	07.29.08	34.231420	-106.679440	31.6	7.77	2950	Williams et al., 2013
East springs	Cibola Spring	05.27.09	34.231440	-106.679340	23.6	7.45	2960	Williams et al., 2013
Coyote	coyote fault well	nr	34.999	-106.470	nr	nr	nr	Williams et al., 2013
Coyote	Coyote Spring	nr	34.99858	-106.47126	12.1	5.7	nr	Williams et al., 2013
Coyote	Coyote Spring	nr	34.99858	-106.47126	10.7	5.9	nr	Williams et al., 2013
Dripping Springs	Dripping Springs	08.22.08	34.416520	-106.475040	22.1	7.73	1471	Williams et al., 2013
Eddlemen	Eddlemen spring	nr	34.785890	-107.40411	17.1	6.9	3660	Williams et al., 2013
West wells	Fish & Wildlife Services Well	05.20.09	34.351450	-106.882510	23.6	7.64	3490	Williams et al., 2013
Four daughters	Four Daughters 2	12.23.09	34.59265	-107.18891	4.10	6.09	38,400	Williams et al., 2013; this study
Four daughters	Four Daughters 3	12.23.09	34.62298	-107.16650	5.20	7.31	58,900	Williams et al., 2013; this study
East springs	Jump Spring	09.04.08	34.153960	-106.750570	20.9	7.2	2200	Williams et al., 2013
SW springs	Ladron Peak Spring 1	10.12.08	34.388210	-107.075380	17.9	7.19	517	Williams et al., 2013
Laguna	Laguna Pueblo 1	11.21.13	34.849992	-107.089483	16.5	6.08	36,700	Williams et al., 2013
East wells	McKensie Well	05.27.09	34.346320	-106.618970	21.6	7.74	587	Williams et al., 2013
Socorro	New Mexico Tech Well	nr	34.073233	-106.945010	25.9	6.89	3990	Williams et al., 2013; this study
Ojo del Abo Spring	Ojo del Abo Spring	07.17.08	34.446945	-106.377780	25	7.42	941	Williams et al., 2013
Rio Salado springs	Rio Salado Box	12.30.04	34.32758	-107.09457	21.3	5.73	5770	Williams et al., 2013
Rio Salado springs	Rio Salado Springs	12.30.04	34.326115	-107.095764	9.6	7.63	5950	Williams et al., 2013
Rio Salado springs	Rio Salado Springs	06.05.09	34.327950	-107.095620	24.3	6.89	5750	Williams et al., 2013
Rio Salado springs	Rio Salado Springs	12.30.04	34.325775	-107.093610	21.3	5.73	5770	Williams et al., 2013
Rio Salado springs	Rio Salado Springs	06.05.09	34.327580	-107.094570	21.9	6.89	5410	Williams et al., 2013
Salado Arroyo	Salado Arroyo	nr	34.697170	-107.122826	6.1	7.3	nr	Williams et al., 2013
San Acacia	San Acacia	01.13.09	34.256410	-106.886960	8.4	7.58	1483	Williams et al., 2013
San Acacia	San Acacia	01.13.09	34.263620	-106.884400	9.6	4.93	23,200	Williams et al., 2013
San Acacia	San Acacia	01.13.09	34.264920	-106.882000	6	4.46	23,300	Williams et al., 2013
West wells	San Acacia Well	nr	34.26373	-106.88452	8.4	7.58	1483	Williams et al., 2013
SW springs	San Lorenzo Spring	07.29.08	34.239150	-107.019780	25.9	8.01	668	Williams et al., 2013
SW springs	San Lorenzo Spring	05.20.09	34.241790	-107.004800	23.8	7.54	943	Williams et al., 2013
SW springs	San Lorenzo Spring	06.05.09	34.238160	-107.021100	23.8	7.75	704	Williams et al., 2013
SW springs	Silver Creek Seep 2	06.05.09	34.289955	-107.034640	25.5	9.42	590	Williams et al., 2013
Socorro	Socorro spring	nr	34.041405	-106.935070	32	7.52	nr	Williams et al., 2013; this study
East wells	Tomasino Well	06.11.09	34.252660	-106.673620	17.5	7.31	756	Williams et al., 2013
West wells	Tule 222 Well	06.04.09	34.412100	-107.000500	22.1	7.39	855	Williams et al., 2013
West wells	West Mesa Well	06.22.09	34.262170	-107.067350	25.1	7.86	327	Williams et al., 2013
Lucero Uplift	Unnamed salt spg	nr	34.698	-107.1207	12	6.4	28,400	Goff et al. 1983
Lucero Uplift	Crane Spg	nr	34.8153	-107.3862	19	7.08	3700	Goff et al. 1983

TABLE 2. Springs' major ions (concentrations in ppm).

ABQ Basin Group	Sample_ID	Spring	Ca	Mg	Na	K	HCO_3	Cl	SO_4	Balance%
Canyon del Ojito Spring	AW080708-SA1	Canyon del Ojito Spring	1.7	0.3	357.3	11.7	291.1	145.5	347.2	-0.7
Canyon del Ojito Spring	AW062409-SA1	Canyon del Ojito Spring	2.0	0.4	341.3	1.7	281.5	127.2	315.0	0.6
East springs	AW052909-CW	Canyon Well	94.0	25.2	38.8	1.6	202.6	10.0	337.3	-12.3
East springs	AW072908-SdC1-1	Cibola Spring	367.4	126.1	95.7	3.1	241.0	21.7	1833.1	-13.0
East springs	AW052709-SdC1-1	Cibola Spring	368.7	166.8	97.7	1.4	248.1	26.0	1640.6	-3.4
Coyote	LC11-NM-CTF-MW2	Coyote fault well	321.6	85.6	534.1	57.8	1842.7	472.0	166.6	0.9
Coyote	DN04-CYS-2	Coyote Spring	169.0	57.5	291.0	27.0	1015.0	432.0	112.0	-8.2
Coyote	DN04-CYS-5	Coyote Spring	251.0	58.8	384.0	25.9	1298.0	516.0	144.0	-5.6
Dripping Springs	AW082208-DS	Dripping Springs	121.6	49.3	100.6	33.7	161.7	34.6	620.0	-4.1
Eddlemen	Eddelman Sp	Eddlemen spring	590.0	135.8	302.5	22.4	553.6	84.6	2009.0	1.1
West wells	AW052009-FWS	Fish & Wildlife Services Well	39.9	33.5	652.0	5.8	174.9	715.3	531.9	-1.3
Four daughters	LC-09-4D-2	Four Daughters 2	389.1	226.6	8000.0	293.4	2385.8	11474.2	3869.6	-5.9
Four daughters	LC-09-4D-3	Four Daughters 3	160.7	254.2	10360.0	324.2	2074.6	15108.6	4720.9	-6.7
East springs	AW090408-JS	Jump Spring	253.9	83.7	51.0	5.5	220.0	15.6	1100.1	-10.4
SW springs	AW101208-LP1	Ladron Peak Spring 1	55.2	13.4	24.6	1.2	257.5	11.5	24.7	-1.3
Laguna	LC13-NM-LAG1	Laguna Pueblo 1	585.6	133.2	8484.0	244.3	3266.9	9306.1	6404.7	-3.9
East wells	AW052709-MW	McKensie Well	36.2	16.4	37.8	2.0	151.5	22.2	39.6	8.1
Socorro	LC10-NM-WTWell-1 & 2	New Mexico Tech Well	112.6	16.9	732.7	30.9	349.0	929.8	203.0	4.6
Ojo del Abo Spring	AW071708-ARS	Ojo del Abo Spring	90.4	42.1	44.2	1.2	526.0	18.6	56.8	-2.1
Rio Salado springs	Rio Salado Box	Rio Salado Box	174.6	49.0	775.0	62.7	403.2	1228.8	547.0	-4.7
Rio Salado springs	DN04-RSB11	Rio Salado Springs	186.1	60.7	729.5	60.9	364.2	1084.6	660.5	-2.9
Rio Salado springs	AW060509-RSB11	Rio Salado Springs	192.9	70.0	693.3	28.4	392.5	1059.1	829.5	-7.4
Rio Salado springs	DN04-RSB12	Rio Salado Springs	174.6	49.0	775.0	62.7	403.2	1228.8	547.0	-4.7
Rio Salado springs	AW060509-RSB12	Rio Salado Springs	155.4	49.0	685.9	28.6	390.5	981.4	592.7	-4.7
Salado Arroyo	DN04-SS-1	Salado Arroyo	269.0	411.0	6440.0	86.5	1324.0	10147.0	3795.0	-8.0
San Acacia	AW011309-SanA-DD	San Acacia	61.2	14.6	185.3	11.2	244.1	181.5	231.3	-5.2
San Acacia	AW011309-SanA-M	San Acacia	524.7	215.6	3717.0	367.0	369.2	5228.3	3475.5	-2.5
San Acacia	AW011309-SanA-S	San Acacia	622.0	228.4	3432.0	96.9	274.6	5147.2	2828.5	-1.7
West wells	San Acacia Well	San Acacia Well	61.2	14.6	185.3	11.2	244.1	181.5	231.3	-5.2
SW springs	AW072908-SLS1	San Lorenzo Spring	20.4	3.7	118.7	2.3	326.4	13.8	45.2	-1.9
SW springs	AW052009-SLS2	San Lorenzo Spring	18.3	13.4	132.4	4.4	343.3	6.9	24.3	10.5
SW springs	AW060509-SLS3	San Lorenzo Spring	46.6	9.9	71.3	3.5	367.7	13.9	38.0	-6.8
SW springs	AW060509-SC2	Silver Creek Seep 2	2.3	0.4	113.3	1.5	310.4	11.4	13.2	-5.6
Socorro	LC10-NM-SocorroSP	Socorro spring	17.8	4.2	66.0	2.6	158.6	13.0	28.6	7.8
East wells	AW061109-TW	Tomasino Well	63.9	29.9	24.6	4.0	319.7	17.1	54.3	-1.8
West wells	AW060409-TUW	Tule 222 Well	36.3	41.5	39.9	3.4	351.1	26.4	84.1	-8.1
West wells	AW062209-WMW	West Mesa Well	11.5	2.1	45.8	2.4	138.3	4.3	21.6	-1.5

Table 3. Carbon isotopic data.

Spring	$\delta^{13}C$	$C_{external}$	$\delta^{13}C_{external}$	% C_{carb}	% C_{org}	% C_{endo}
Canyon del Ojito Spring	-5.31	0.004	-5.3	0.3	26.8	72.9
Canyon del Ojito Spring	-4.70	0.004	-4.7	0.3	24.8	74.8
Canyon Well	-5.50	0.003	-8.5	28.8	26.5	44.7
Cibola Spring	-7.99	bdl	nr	130.7	31.2	-61.9
Cibola Spring	-8.30	bdl	nr	160.3	31.3	-91.6
coyote fault well	-2.2	0.026	-3.8	27.5	15.9	56.6
Coyote Spring	-5.00	0.087	-5.4	5.9	25.6	68.5
Coyote Spring	-4.10	0.075	-4.7	8.7	22.6	68.7
Dripping Springs	-2.13	0.001	-14.2	74.5	14.1	11.3
Eddlemen spring	2.92	0.006	3.8	49.9	0.0	50.1
Fish & Wildlife Services Well	-5.34	0.002	-11.7	46.4	25.4	28.2
Four Daughters 2	-4	0.092	-4.6	9.4	22.3	68.3
Four Daughters 3	-4	0.027	-6.4	28.4	21.7	49.9
Jump Spring	-7.91	0.001	-66.5	85.5	32.4	-18.0
Ladron Peak Spring 1	-12.20	0.003	-19.7	34.6	47.9	17.5
Laguna Pueblo 1	-8.5	0.115	-9.0	4.7	36.9	58.4
McKensie Well	-5.72	0.001	-12.2	45.5	26.7	27.8
New Mexico Tech Well 1	-3.0	0.006	-4.2	19.8	5.1	75.1
New Mexico Tech Well 2	-5.9	0.006	-7.8	19.8	16.5	63.7
Ojo del Abo Spring	-10.81	0.006	-18.3	36.9	43.4	19.8
Rio Salado Box	-4.29	0.027	-4.8	6.9	23.3	69.8
Rio Salado Springs	0.81	0.004	0.0	39.9	5.8	54.3
Rio Salado Springs	-2.55	0.005	-5.2	36.6	16.7	46.7
Rio Salado Springs	-4.29	0.027	-4.8	6.9	23.3	69.8
Rio Salado Springs	-0.60	0.006	-1.5	25.5	10.8	63.7
Salado Arroyo	-1.00	0.007	-8.5	71.6	10.6	17.8
San Acacia	-8.03	0.004	-9.7	14.1	35.1	50.7
San Acacia	-4.75	0.133	-5.2	6.3	24.8	68.9
San Acacia	-3.99	0.326	-4.2	2.8	22.5	74.7
San Acacia Well	-13.7	0.004	-16.3	14.1	53.4	32.5
San Lorenzo Spring	-10.22	0.005	-10.7	3.6	42.5	53.9
San Lorenzo Spring	-16.54	0.005	-19.2	12.7	62.6	24.7
San Lorenzo Spring	-11.22	0.005	-14.3	18.9	45.3	35.8
Silver Creek Seep 2	-10.88	0.004	-10.9	0.3	44.8	54.9
Socorro Spring	-3.6	0.008	-3.8	4.0	4.6	91.4
Tomasino Well	-5.7	0.004	-10.6	39.0	26.8	34.2
Tule 222 Well	-3.5	0.004	-5.6	27.9	20.1	52.0
West Mesa Well	-4.8	0.002	-5.3	6.5	25.0	68.6

Group basin-fill aquifer system, Mesozoic aquifers, Paleozoic carbonate and sandstone aquifers, and from basement penetrating faults that can convey deep fluids.

METHODS

The multiple tracer method evaluates mixing end members and allows for inferences regarding fluid sources and mixing. Consistency among tracers such as general chemistry, gas abundance, and isotopes of carbon is explored. Major ions identify locations with increased salinity and evidence for water-rock interaction. Gas abundance data, in particular dissolved N_2-Ar-He, display the range of gas results from helium-rich endogenic gases to air and air-saturated water and can also show mixing patterns (Giggenbach et al., 1992; Newell et al., 2005).

In the field, the spring temperature, pH, conductivity and total dissolved solids were measured using an Oakton meter. Two Nalgene 125-mL bottles were collected at each spring. The first bottle was collected without head space for preserving alkalinity; water from this bottle was used to measure anions and carbon isotopes. The spring water for the second bottle was filtered with a 0.45-micron filter and acidified with HNO_3 to preserve dissolved metals and cations. Gas samples were collected with two methods (1) by placing a plastic funnel over bubbling springs and drawing the gases into an evacuated glass flask or glass bottle filled with concentrated NaOH, or (2) water samples were drawn into an evacuated and NaOH-filled container and then gases were extracted out of solution (Newell et al., 2005).

Water analyses were run in the Analytical Laboratory of the Earth and Planetary Department of the University of New Mexico. Alkalinity was determined by titration with sulfuric acid. The anions were analyzed using an ion chromatographer (EPA Method 300.1, Revision 1.0, Hautman and Munch, 1997), and cations were analyzed with an inductively coupled plasma optical emission spectrometry (EPA Method 200.7, Revision 4, Creed, et al., 1994). Gas samples were analyzed for He, H_2, Ar, N_2, O_2, CH_4, and CO with a gas chromatograph after Giggenbach and Goguel (1989) in the University of New Mexico Volcanic Geothermal Fluid Analysis Laboratory.

Our method to help quantify the components of the CO_2 load is summarized in Chiodini et al., (2004) and Crossey et al. (2009). Three potential sources of carbon within groundwater are identified: (1) C_{carb}= carbon derived from dissolving carbonates (both rock and minerals) in the aquifer system, for example from limestone aquifers like the Madera Group and San Andres Formation, (2) C_{org}= carbon derived from organic sources such as soil gas derived from plant respiration, and (3) C_{endo}= carbon derived from endogenic (deeply derived) sources such as magmatic volatile inputs or CO_2 released by ascending geothermal fluids below the aquifer system. The method for estimating the proportions of these components relies first on major element chemistry of the water, and then carbon isotope data.

First, the total dissolved inorganic carbon (DIC) is modeled with PHREEQC using major ion chemistry and pH (Parkhurst, 1995). The modeled DIC is a combination of the titratable bicarbonate (HCO_3^-) and carbonic acid (H_2CO_3). Considering the percentage of carbonic acid is especially important for springs

Table 4. Dissolved gas chemistry data.

Spring	Ar %	He %	O_2 %	*CO_2 %	H_2 %	H_2S %	N_2 %	CH_4 %	Source
Comanche Fault Spr - Salado arroyo	0.87	<1.84E-03	17.7	0.071	0.004	2.110	72.1	<4.43E-04	Newell et al., 2005
Comanche Fault Spr - Salado arroyo stream	0.76	0.02	16.8	19.9	0.011	bd	62.6	<4.16E-04	Newell et al., 2005
Coyote fault well	0.004	0.002	0.0	21.5	nr	nr	0.2	5.43E-04	William et al., 2013
Coyote fault well short sample	0.003	0.04	nr	19.5	nr	nr	0.2	7.82E-05	William et al., 2013
Coyote Spring 1	0.55	<1.15E-03	10.8	43.2	0.004	bd	45.5	<2.78E-04	Newell et al 2005
Coyote Spring 2	0.07	0.001	1.7	92.1	0.001	bd	6.14	<3.38E-05	Newell et al., 2005
Eddleman Spring	<2.26E-04	<1.67E-04	<2.19E-04	99.1	0.001	bd	0.887	5.53E-03	Newell et al., 2005
Eddleman Spring	nr	nr	nr	86.0	nr	nr	nr	0.185	William et al., 2013
Four Daiughters Spring	0.01	1.64E-06	nr	12.5	nr	nr	0.37	1.33E-01	William et al., 2013; this study
New Mexico Tech Well 1	0.0193	1.28E-02	nr	1.9	nr	nr	0.82	nr	William et al., 2013; this study
New Mexico Tech Well 2	0.0302	1.02E-02	nr	1.51	nr	nr	1.176	nr	William et al., 2013; this study
Rio Salado Box spring	nr	nr	nr	6.4	nr	nr	nr	6.70E-03	William et al., 2013
Salado Arroyo Spr	0.783	0.006	15.90	18.6	0.006	bd	64.7	<4.25E-04	Newell et al., 2005
Salado Arroyo Spring	nr	nr	nr	92.4	nr	nr	nr	nr	William et al., 2013
San Acacia puddle	nr	nr	nr	24.5	nr	nr	nr	0.258	William et al., 2013
San Acacia spring	nr	nr	nr	2.7	nr	nr	nr	nr	William et al., 2013
Socorro spring	1.95	9.20E-06	nr	10.01	nr	nr	0.793	nr	William et al., 2013; this study
Tunnel Spring – Sandia Pk	0.95	<2.04E-03	6.97	13.8	0.008	bd	78.30	<4.93E-04	Newell et al., 2005

* CO_2 is water-free (Newell et al., 2005)

with a pH below 6.5. The C_{carb} is calculated via

$$C_{carb} = Ca + Mg\text{-}SO_4.$$

The molar balance of Ca + Mg accounts for CO_2 released from dissolution of calcite and dolomite (Ca, Mg, CO_3), and the –SO_4 term accounts for any extra Ca and Mg that may have come from dissolution of gypsum (Ca, Mg, SO_4). The remaining carbon is called external carbon such that

$$C_{ext} = DIC_{total} - C_{carb},$$

and is composed of two end members C_{org} and C_{endo} ($C_{ext} = C_{org} + C_{endo}$).

Carbon isotopes and C_{ext} concentrations were used to create a mixing curve between C_{org} and C_{endo} end members, allowing us to estimate their relative contributions. Before creating this mixing curve, the concentrations and isotopes must be corrected for carbonate contributions; the $\delta^{13}C$ of external carbon is adjusted with the equation

$$(\delta^{13}C_{ext} * C_{ext}) = (\delta^{13}C_{DIC} * DIC) - (\delta^{13}C_{carb} * C_{carb}).$$

The final step is defining a set of mixing curves that envelop the data and help define isotopic values of the end members. For example, for soil gas respiration sources, an organic end member ranges from -22 to -34‰ for C3 plants and -9 to -16‰ for C4 plants (Robinson and Scrimgeour, 1995). Possible values for the carbon isotope endogenic end member at high C_{ext} were bracketed empirically by our data. Published ranges of $\delta^{13}C$ of mantle carbon are reported in Goff et al., (2000) as -3.5‰, by Gerlach and Taylor (1990) as -4.1 to -3.5‰ and by Sano and Marty (1995) at -6±2‰.

RESULTS

Major ion chemistry is presented in a Piper diagram (Piper, 1944) in Figure 3. The diagram displays cations in the lower left triangle and the anions in the lower right, and the ions are then projected into the parallelogram. Epigenic waters fall near the left apex of parallelogram. The Albuquerque basin waters also plot in each corner of the parallelogram and these were interpreted by Williams et al. (2013) to represent different endogenic endmembers. The springs with highest endogenic input tend to plot near the Na-SO_4 (right apex) corner. As shown in Figure 3, these springs correspond to the "type-s" (saline mineral waters) of Goff et al. (1983). Springs near the top of the parallelogram are similar to their "type-d" waters (dilute mineral waters).

Results from the C_{ext} calculations (Fig. 4) show that most carbonic springs fall on binary mixing curves between C_{org} and C_{endo}, with endogenic end members of $\delta^{13}C_{ext}$ = -3.5 to 6‰ and [C_{ext}]= 0.03 to 0.32 mol/L. The C_{ext} diagram can be used to estimate carbon proportions for each sample as shown in Table 3 and Figure 5. C_{endo} dominates the carbon proportion for most samples and the overall average for the carbonic springs of the ABQ basin is:

$$C_{carb} = 22.9\% \pm 21.4\%,$$
$$C_{org} = 22.6\% \pm 11.6\%, \text{ and}$$
$$C_{endo} = 55.3\% \pm 19.8\%.$$

Results of our new gas analyses are similar to what was reported by Newell et al. (2005) where gas chemistry, in particular for Salado Arroyo springs, shows a wide spectrum of mixing between a helium-rich endogenic end-member in lower left corner and air or air-saturated water on the right axis (Fig. 6).

IMPLICATIONS AND DISCUSSION

The multiple tracer method shows similar trends among hydrochemistry, carbon isotopes and gas chemistry. Springs that lie along a mixing line from meteoric (Ca-Mg-HCO_3-Cl) to endogenic (Na-SO_4) end members in the Piper diagram (Fig. 3)

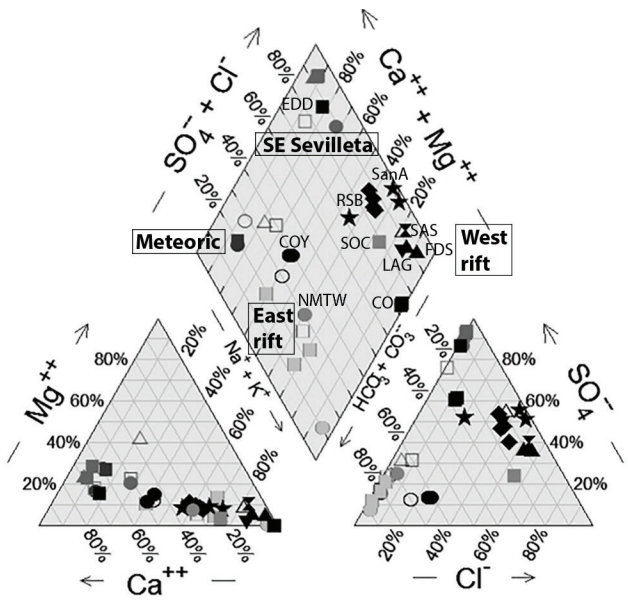

FIGURE 3. Piper diagram projects cation and anion triangles in lower part of the diagram into central parallelogram and shows three mixing trends for epigenic and endogenic mixing, with the epigenic end member, Ca-HCO_3, shown in the left corner of the parallelogram and three different endogenic end-members shown in the remaining three corners. The western and central rift carbonic springs and Coyote springs along the Tijeras fault are mostly Na-SO_4 waters. The next endogenic end member is Ca-SO_4, present in the Eddlemen spring of the Colorado Plateau and southeast Sevilleta springs. The last endogenic member is Na-HCO_3, found in the southwestern Sevilleta springs. This paper is mainly interested in the Na-SO_4 and Na-Cl endogenic end member, which is interpreted to reflect input of magmatic volatiles from the Socorro magma body. Springs displayed as small black dots are from Goff et al. (1983); these springs plot in all three endogenic water types on the Piper diagram and provide supporting evidence of complex mixing among multiple geothermal end members.

also have $\delta^{13}C_{ext}$ values around -5‰, typical of deeply sourced CO_2, as shown in the C_{ext} plot (Fig. 4). Among these springs the highest concentrations of endogenic carbon are at San Acacia Spring with 0.33 mol/L, Four Daughters with 0.09 mol/L and Salado Arroyo springs with 0.027 mol/L. These springs also have high conductivities: San Acacia has 23,000 µS, Four Daughters has 38,000 to 59,000 µS and Salado Arroyo has 5950 µS. In the non-reactive gas plot (Fig. 6), results from Salado Arroyo springs creates a mixing line between helium-rich to air-like gases. The other gas sample plotted is Four Daughters spring, which plots close to air-saturated water.

The chemical tracers in the carbonic springs of the Albuquerque basin plot along linear trends in each figure (Piper, carbon isotopes, and dissolved gases) implying mixing among end members. The linear trends extend toward accepted endogenic values. Pure endogenic endmember fluids, for example gases from the mantle, are not available to sample, but the consistency among tracers supports the hypothesis of mixing between epigenic and endogenic end members.

The linear mixing patterns shown in the Albuquerque basin springs are similar to the mixing trends of the Socorro spring and New Mexico Tech well from Williams et al. (2013). Similarities include Na-SO_4 as the dominate ions and $\delta^{13}C$ values around -4 to -5‰. Socorro waters are different from the Albuquerque basin because they are lower in external carbon concentrations at 0.006 mol/L. According to non-reactive gases (Fig. 6), Socorro waters plot along the helium-rich to air-saturated water end members, clearly showing endogenic He additions.

Western rift margin waters suggest a mixing trend involving endogenic waters. This region overlies the Socorro magma body and the Socorro seismic anomaly (Fig. 1). The Socorro magma body may be the source of endogenic input in the Albuquerque Basin springs, and the Socorro seismic anomaly may help fluids flow upwards along faults. The conduit system for ascent of endogenic fluids likely involves basaltic magmas originating as partial melt from the mantle, CO_2 degassing from above the magma body, interaction with basin

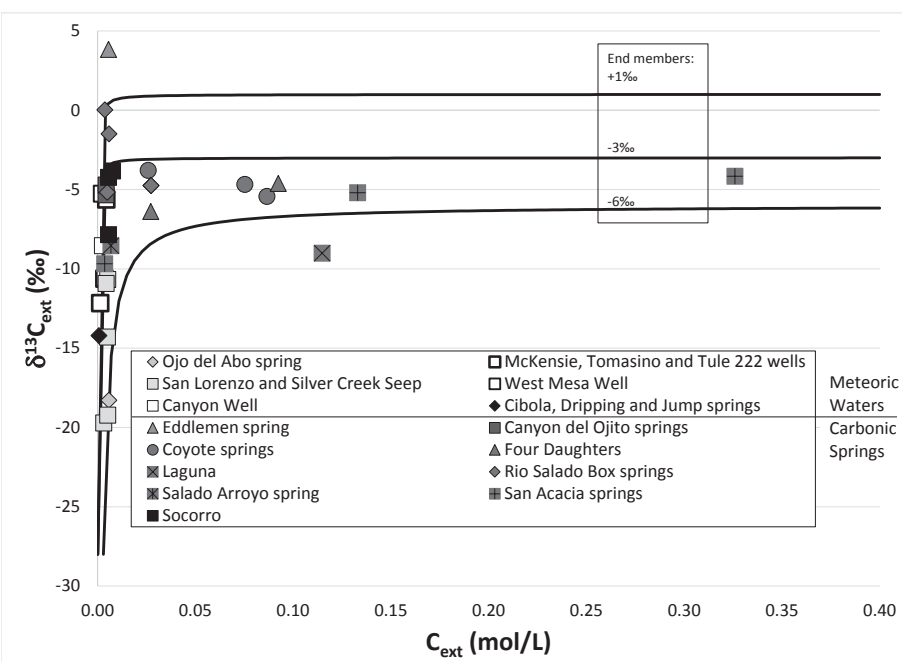

FIGURE 4. C_{ext} (concentration of external carbon) plotted versus $\delta^{13}C$ (of C_{ext}) allows calculation of C_{org} versus C_{endo} components of the C_{ext}. External carbon is the concentration of only the organic and endogenic sources of carbon, in other words the carbon from dissolution of carbonates is subtracted out. This figure shows binary mixing curves between C_{org} (at -28‰ and low concentrations of external carbon) and C_{endo} (ranging from -3 to -6‰, with high concentrations of external carbon). The springs with the highest concentration of C_{ext} are Laguna (LAG), Four Daughters (FDS) and Rio Salado Box (RSB) along the western rift faults, San Acacia (SanA) along the Cliff fault, and Coyote (COY) at the intersection of the Sandia and Tijeras fault zones. The carbonic western rift-flank springs have $\delta^{13}C$ values around -5‰, a typical endogenic end member.

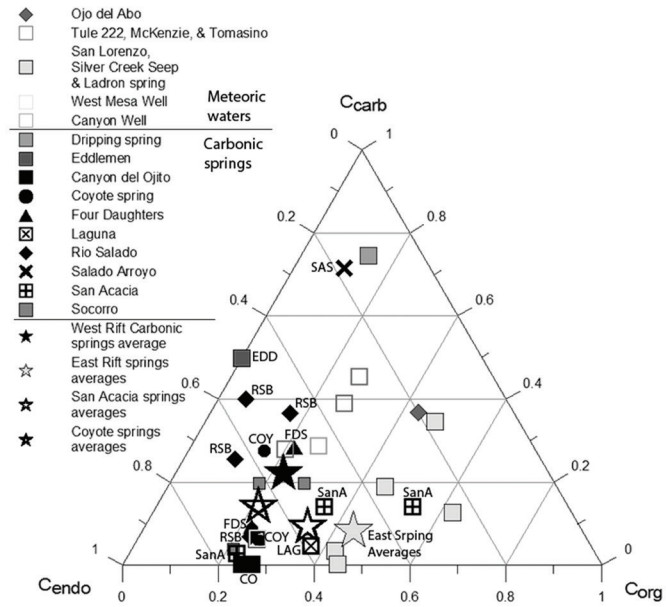

FIGURE 5. Triangular plot of the carbon sources for each spring derived from the C_{ext} (external carbon) analysis (see figure 4 caption). Western rift springs Laguna (LAG), Four Daughters (FDS), Rio Salado Box (RSB), Canyon del Ojito (CO), Salado Arroyo (SAS) range from 17.5 to 74.8% endogenic carbon.

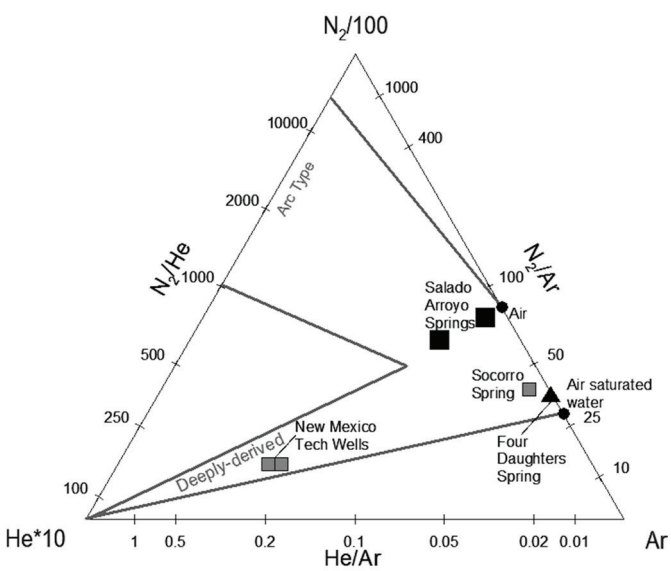

FIGURE 6: Trilinear plot of non-reactive gases in different springs. The non-reactive gases, Ar-N_2-He, create a mixing line from endogenic (helium rich) to epigenic gases (air and air saturated water). Air and air-saturated waters have trace concentrations of helium compared to Ar and N_2, and are defined by their N_2/Ar ratios.

brines, upward ascent on faults, and near-surface degassing of CO_2 around spring vents that causes deposition of travertine (Crossey et al., 2016).

The high CO_2 in the endogenic fluids is interpreted to be derived in part from the Socorro Magma body. This is not incompatible with the finding of Goff et al. (1983) based on chemical geothermometers that waters along the Comanche fault (their S-type waters) equilibrated at temperatures of less than 30-60°C and groundwaters of the Lucero uplift (their D-type waters) equilibrated at temperatures of <30°C. Based on current data, we agree with their conclusion that these waters have little potential for geothermal electricity generation, but that inputs of geothermal water helps explain the hydrochemistry and that geothermal direct use potential may be present.

CONCLUSIONS

The results show that endogenic volatiles and solutes are present in springs on both sides of the Rio Grande rift and on intra-rift faults. These spring waters are dominated by Na-SO_4, high concentration of endogenic carbon and $\delta^{13}C_{ext}$ values around -5‰. We suggest the CO_2 along the west flank of the rift of the Albuquerque basin was derived in part from magmatic degassing of the Socorro magma body that likely affects a large region beneath west flank springs, including the Socorro spring and New Mexico Tech well. This paper shows the importance of studying tectonic controls on spring water chemistry because it highlights the need to better understand the influence of even small volumes of geothermal fluids on regional groundwater and mixing processes within the deep aquifer.

ACKNOWLEDGMENTS

Funding came from the Hydrologic Sciences Program of the National Science Foundation (NSF EAR 0538304 and 0838575 to Crossey and Karlstrom), the National Science Foundation grant to the University of New Mexico for long term Ecological Research (NSF-DEB-0620482 to Collins) at the Sevilleta National Wildlife Refuge, and NM EPSCoR grants 0814449 and 11A-1301346.

REFERENCES

Callender, J.F., and Zilinski, R.E., 1976, Kinematics of Tertiary and Quaternary deformation along the eastern edge of the Lucero uplift, central New Mexico: New Mexico Geological Society Special Publications, v. 6, p. 53-61.

Chapin, C.H., and Cather, S.M., 1994, Tectonic setting of the axial basin of the northern and central Rio Grande rift: Geologic Society of America Special Papers, v. 291, p. 5-26.

Chiodini, G., Cardellini, C., Amato, A., Boschi, E., Caliro, S., Frondini, F., and Ventura, G., 2004, Carbon dioxide Earth degassing and seismogenesis in central and southern Italy: Geophysical Research Letters, v. 31, p. 1-4.

Creed, J. T., Brockhoff, C. A., and Martin, T. D., 1994, Method 200.8: Determination of trace elements in waters and wastes by inductively-coupled plasma-mass spectrometry. Environmental Monitoring Systems Laboratory, Office of Research and Development, US Environmental Protection Agency, Cincinnati, OH, Rev, 5.

Crossey, L.J., Fischer, T.P., Patchett, P.J., Karlstrom, K.E., Hiton, D.R., and Newell, D.L., Huntoon, P., Reynolds, A.C., and de Leeuw, G.A.M., 2006, Dissected hydrologic system at the Grand Canyon: Interaction between deeply derived fluids and plateau aquifer waters in modern springs and travertine: Geological Society of America, v. 34, no. 1, p. 25-28.

Crossey, L.J., Karlstrom, K.E., Springer, A.E., Newell, D., Hilton, D.R., and Fischer, T., 2009, Degassing of mantle-derived CO_2 and He from springs in the southern Colorado Plateau region – Neotectonic connections and implications for groundwater systems: Geological Society of America Bulletin, v. 121, no. 7-8, p. 1034-1053.

Crossey, L.J., Karlstrom, K.E., Newell, D.L., Kooser, A., and Tafoya, A., 2011, The La Madera Travertines, Rio Ojo Caliente, northern New Mexico:

Investigating the linked system of CO_2-rich springs and travertines as neotectonic and paleoclimate indicators: New Mexico Geological Society, Guidebook 62, p. 301-316.

Crossey, L.J., Karlstrom, K.E., Schmandt, B., Crow, R.R., Colman, D.R., Cron, B., Takacs-Vesbach, C.D., Dahm, C.N., Northup, D.E., Hilton, D.R., Ricketts, J.W., and Lowry, A.R., 2016, Continental smokers couple mantle degassing and distinctive microbiology within continents: Earth and Planetary Science Letters, v. 435, p. 22-30.

Fournier, R.O., and Truesdell, A.H., 1973, An empirical Na-K-Ca geothermometer for natural waters: Geochimica et Cosmochimica Acta, v. 37, p. 1255-1275.

Gerlach, T.M. and Taylor, B.E., 1990, Carbon isotope constraints on degassing of carbon dioxide from Kilauea Volcano: Geochimica et Cosmochimica Acta, v. 54, p. 2051-2058.

Giggenbach, W.F., and Goguel, R.L., 1989, Methods for the collection and analysis of geothermal and volcanic water and gas samples: Department of Scientific and Industrial Research, Chemistry Division, Report, 2401.

Giggenbach, W.F., 1992, The composition of gases in geothermal and volcanic systems as a function of tectonic setting: Water-Rock Interaction, v. 82, p. 873-878.

Goff, F., McCormick, T., Gardner, J.N., Trujillo, P.E., Counce, D., Vidale, R., and Charles, R., 1983, Water geochemistry of the Lucero uplift, New Mexico: A geothermal investigation of low-temperature mineralized fluids: Los Alamos National Laboratory, NM, No. LA-9738-OBES.

Goff, F., McMurtry, G.M., Counce, D., Simac, J.A., Roldan-Manzo, A.R., and Hilton, D.R., 2000, Contrasting hydrothermal activity at Sierra Negra and Alcedo volcanos, Galapagos Archipelago, Ecuador: Bulletin of Volcanology, v. 62, p. 34-52.

Grauch, V.J.S., Connel, S.D., Ferguson, J., and McIntosh, W., 2013, Structure and tectonic evolution of the eastern Espanola Basin, Rio Grande rift, north-central New Mexico: Geological Society of America Special Papers, v. 495, p. 185-219.

Hautman, D.P., and Munch, D.J., 1997, Method 300.1 Determination of inorganic anions in drinking water by ion chromatography, Revsion 1.0: National Exposure Research Laboratory Office of Research and Development U.S. Environmental Protection Agency Cincinnati, OH 45268.

Hogan, J.F., Phillips, F.M., Mills, S.K., Hendrickx, J.M.H., Ruiz, J., Chesley, J.T., and Asmerom, Y., 2007, Geologic origins of salinization in a semi-arid river: the role of sedimentary basin brines: Geology, v. 35, p. 1063–1066.

Keller, G.R., and Baldridge, W.S., 1999, The Rio Grande rift: A geological and geophysical overview: GeoScience World, v. 34, p. 121-130.

Lewis, C.J., and Baldridge, W.S., 1994, Crustal extension in the Rio Grande rift, New Mexico: Half-grabens, accommodation zones, and shoulder uplifts in the Ladron Peak-Sierra Lucero area: Geological Society of America Special Papers, v. 291, p. 135-156.

Mills, S.K., 2003, Quantifying salinization of the Rio Grande using environmental tracers [M.S. Thesis]: Socorro, New Mexico Institute of Mining and Technology, 397 p.

Newell, D.L., Crossey, L.J., Karlstrom, K.E., Fischer, T.P., and Hilton, D.R., 2005, Continental-scale links between the mantle and groundwater systems of the western United States: Evidence from travertine springs and regional He isotope data: GSA Today, v. 15, no. 12, p. 4-11.

Parkhurst, D.L., 1995, User's guide to PHREEQC—A computer program for speciation, reaction-path, advective-transport, and inverse geochemical calculations: U.S. Geological Survey Water Resources Investigations Report, 95-4227, 143 p.

Piper, A., 1944, A graphic procedure in the geochemical interpretation of water-analysis: Eos, Transactions American Geophysical Union, v. 25, p. 914-928.

Priewisch, A., Crossey, L.J., Karlstrom, K.E., Polyak, V.J., Asmerom, Y., Nereson, A., and Ricketts, J.W., 2014, U-Series geochronology of the southeastern Colorado Plateau: Evaluating episodicity and tectonic and paleohydrologic controls: Geosphere, v. 10 p. 401-423.

Ricketts, J.W., Karlstrom, K.E., Priewisch, A., Crossey, L.J., Polyak, V.J., and Asmerom, Y., 2014, Quaternary extension in the Rio Grande rift at elevated strain rates recorded in travertine deposits, central New Mexico: Lithosphere, v. 6, p. 3-16.

Robinson, D., and Scrimgeour, C.M., 1995, The contribution of plant C to soil CO_2 measured using $\delta^{13}C$: Soil Biology and Biogeochemistry, v. 27, p. 1653– 1656.

Russell, L.R., and Snelson, S., 1994, Structure and tectonics of the Albuquerque basin segment of the Rio Grande rift: Insights from reflection seismic data: Geological Society of America Special Papers, v. 291, p. 83-112.

Sano, Y. and Marty, B., 1995, Origin of carbon in fumarolic gas from island arcs: Chemical Geology, v. 119, p. 265–274.

Trainer, F.W., and Lyford, F.P., 1979, Geothermal hydrology in the Rio Grande rift, north central New Mexico: New Mexico Geological Society, Guidebook 30, p. 299-306.

Williams, A.J., Crossey, L.J., Karlstrom, K.E., Newell, D., Person, M., and Woolsey, E., 2013, Hydrochemistry of the Middle Rio Grande aquifer system – Fluid mixing and salinization of the Rio Grande due to fault inputs: Chemical Geology, v. 351, p. 281–298.

Travertine dams. Photo courtesy of Peter Scholle.